Broad-band continuous-wave parametric wavelength conversion in silicon nanowaveguides

Mark A. Foster[1], **Amy C. Turner**[2], **Reza Salem**[1], **Michal Lipson**[2], **and Alexander L. Gaeta**[1]

[1]*School of Applied and Engineering Physics, Cornell University, Ithaca, NY 14853*
[2]*School of Electrical and Computer Engineering, Cornell University, Ithaca, NY 14853*
alg3@cornell.edu

Abstract: We demonstrate highly broad-band frequency conversion via four-wave mixing in silicon nanowaveguides. Through appropriate engineering of the waveguide dimensions, conversion bandwidths greater than 150 nm are achieved and peak conversion efficiencies of -9.6 dB are demonstrated. Furthermore, utilizing fourth-order dispersion, wavelength conversion across four telecommunication bands from 1477 nm (S-band) to 1672 nm (U-band) is demonstrated with an efficiency of -12 dB.

OCIS codes: (190.4380) Four-wave mixing; (130.5990) Semiconductors; (130.4310) Nonlinear; (130.3060) Infrared

References and links

1. H. K. Tsang, C. S. Wong, T. K. Liang, I. E. Day, S. W. Roberts, A. Harpin, J. Drake, M. Asghari, "Optical dispersion, two-photon absorption and self-phase modulation in silicon waveguides at 1.5 μm wavelength," Appl. Phys. Lett. **80**, 416 (2002).
2. M. Dinu, F. Quochi, H. Garcia, "Third-order nonlinearities in silicon at telecom waveguides," Appl. Phys. Lett. **82**, 2954 (2003).
3. T. Liang, L. Nunes, T. Sakamoto, K. Sasagawa, T. Kawanishi, M. Tsuchiya, G. Priem, D. Van Thourhout, P. Dumon, R. Baets, H. Tsang, "Ultrafast all-optical switching by cross-absorption modulation in silicon wire waveguides," Opt. Express **13**, 7298 (2005), http://www.opticsinfobase.org/abstract.cfm?URI=oe-13-19-7298.
4. R. A. Soref, B. R. Bennett, "Electrooptical effects in silicon," IEEE J. Quantum Electron. **23**, 123 (1987).
5. V. R. Almeida, C. A. Barrios, R. R. Panepucci, and M. Lipson, "All-optical control of light on a silicon chip," Nature **431**, 1081 (2004).
6. R. Claps, D. Dimitropoulos, Y. Han, B. Jalali, "Observation of Raman emission in silicon waveguides at 1.54 m," Opt. Express **10**, 1305 (2002), http://www.opticsexpress.org/abstract.cfm?URI=OPEX-10-22-1305.
7. R. Claps, D. Dimitropoulos, B. Jalali, "Stimulated Raman scattering in silicon waveguides," IEEE Electron. Lett. **38**, 1352 (2002).
8. R. Claps, D. Dimitropoulos, V. Raghunathan, Y. Han, B. Jalali, "Observation of stimulated Raman amplification in silicon waveguides," Opt. Express **11**, 1731 (2003), http://www.opticsinfobase.org/abstract.cfm?URI=oe-11-15-1731.
9. R. Jones, H. Rong, A. Liu, A. Fang, M. Paniccia, D. Hak, O. Cohen, "Net continuous wave optical gain in a low loss silicon-on-insulator waveguide by stimulated Raman scattering," Opt. Express **13**, 519 (2005), http://www.opticsinfobase.org/abstract.cfm?URI=oe-13-2-519.
10. H. Rong, A. Liu, R. Jones, O. Cohen, D. Hak, R. Nicolaescu, A. Fang, M. Panniccia, "An all-silicon Raman laser," Nature **433**, 292 (2005).
11. H. Rong, R. Jones, A. Liu, O. Cohen, D. Hak, A. Fang, M. Paniccia, "A continuous-wave Raman silicon laser," Nature **433**, 725, (2005).
12. Y. Okawachi, M. Foster, J. Sharping, A. Gaeta, Q. Xu, M. Lipson, "All-optical slow-light on a photonic chip," Opt. Express **14**, 2317 (2006), http://www.opticsinfobase.org/abstract.cfm?URI=oe-14-6-2317.

#84176 - $15.00 USD Received 15 Jun 2007; revised 13 Aug 2007; accepted 13 Aug 2007; published 24 Sep 2007

13. O. Boyraz, T. Indukuri, B. Jalali, "Self-phase-modulation induced spectral broadening in silicon waveguides," Opt. Express **12**, 829 (2004), http://www.opticsinfobase.org/abstract.cfm?URI=oe-12-5-829.
14. A. Cowan, G. Rieger, J. Young, "Nonlinear transmission of 1.5 μm pulses through single-mode silicon-on-insulator waveguide structures," Opt. Express **12**, 1611 (2004), http://www.opticsinfobase.org/abstract.cfm?URI=oe-12-8-1611.
15. O. Boyraz, P. Koonath, V. Raghunathan, B. Jalali, "All optical switching and continuum generation in silicon waveguides," Opt. Express **12**, 4094 (2004), http://www.opticsinfobase.org/abstract.cfm?URI=oe-12-17-4094.
16. J. E. Sharping, K. F. Lee, M. A. Foster, A. C. Turner, B. S. Schmidt, M. Lipson, A. L. Gaeta, P. Kumar, "Generation of correlated photons in nanoscale silicon waveguides," Opt. Express **14**, 12388-12393 (2006), http://www.opticsinfobase.org/abstract.cfm?URI=oe-14-25-12388.
17. E. Dulkeith, Y. A. Vlasov, X. Chen, N. C. Panoiu, R. M. Osgood, "Self-phase-modulation in submicron silicon-on-insulator photonic wires," Opt. Express **14**, 5524 (2006), http://www.opticsinfobase.org/abstract.cfm?URI=oe-14-12-5524.
18. I. -W. Hsieh, X. Chen, J. I. Dadap, N. C. Panoiu, R. M. Osgood, S. J. McNab, Y. A. Vlasov, "Ultrafast-pulse self-phase modulation and third-order dispersion in Si photonic wire-waveguides," Opt. Express **14**, 12380 (2006), http://www.opticsinfobase.org/abstract.cfm?URI=oe-14-25-12380.
19. R. Dekker, A. Driessen, T. Wahlbrink, C. Moormann, J. Niehusmann, M. Forst, "Ultrafast Kerr-induced all-optical wavelength conversion in silicon waveguides using 1.55 m femtosecond pulses," Opt. Express **14**, 8336 (2006), http://www.opticsinfobase.org/abstract.cfm?URI=oe-14-18-8336.
20. I. -W. Hsieh, X. Chen, J. I. Dadap, N. C. Panoiu, R. M. Osgood, S. J. McNab, Y. A. Vlasov, "Cross-phase modulation-induced spectral and temporal effects on co-propagating femtosecond pulses in silicon photonic wires," Opt. Express **15**, 1135 (2007), http://www.opticsinfobase.org/abstract.cfm?URI=oe-15-3-1135.
21. D. Dimitropoulos, V. Raghunathan, R. Claps, B. Jalali, "Phase-matching and nonlinear optical processes in silicon waveguides," Opt. Express **12**, 149 (2004), http://www.opticsinfobase.org/abstract.cfm?URI=oe-12-1-149.
22. V. Raghunathan, R. Claps, D. Dimitropoulos, B. Jalali, "Parametric Raman wavelength conversion in scaled silicon waveguides," J. Lightwave Technol. **23**, 2094 (2005).
23. R. L. Espinola, J. I. Dadap, R. M. Osgood, S. J. McNab, Y. A. Vlasov, "C-band wavelength conversion in silicon photonic wire waveguides," Opt. Express **13**, 4341 (2005), http://www.opticsinfobase.org/abstract.cfm?URI=oe-13-11-4341.
24. H. Fukuda, K. Yamada, T. Shoji, M. Takahashi, T. Tsuchizawa, T. Watanabe, J. Takahashi, S. Itabashi, "Four-wave mixing in silicon wire waveguides," Opt. Express **13**, 4629 (2005), http://www.opticsinfobase.org/abstract.cfm?URI=oe-13-12-4629.
25. H. Rong, Y. -H. Kuo, A. Liu, M. Paniccia, O. Cohen, "High efficiency wavelength conversion of 10 Gb/s data in silicon waveguides," Opt. Express **14**, 1182 (2006), http://www.opticsinfobase.org/abstract.cfm?URI=oe-14-3-1182.
26. M. A. Foster, A. C. Turner, J. E. Sharping, B. S. Schmidt, M. Lipson, A. L. Gaeta, "Broad-band optical parametric gain on a silicon photonic chip," Nature **441**, 960 (2006).
27. K. Yamada, H. Fukuda, T. Tsuchizawa, T. Watanabe, T. Shoji, S. Itabashi, "All-optical efficient wavelength conversion using silicon photonic wire waveguide," IEEE Photon. Technol. Lett. **18**, 1046 (2006).
28. Q. Lin, J. Zhang, P. M. Fauchet, G. P. Agrawal, "Ultrabroadband parametric generation and wavelength conversion in silicon waveguides," Opt. Express **14**, 4786 (2006), http://www.opticsinfobase.org/abstract.cfm?URI=oe-14-11-4786.
29. Y. -H. Kuo, H. Rong, V. Sih, S. Xu, M. Paniccia, O. Cohen, "Demonstration of wavelength conversion at 40 Gb/s data rate in silicon waveguides" Opt. Express **14**, 11721 (2006), http://www.opticsinfobase.org/abstract.cfm?URI=oe-14-24-11721.
30. L. Yin, Q. Lin, G. P. Agrawal, "Dispersion tailoring and soliton propagation in silicon waveguides," Opt. Lett. **31**, 1295 (2006).
31. E. Dulkeith, F. Xia, L. Schares, W. M. J. Green, Y. A. Vlasov, "Group index and group velocity dispersion in silicon-on-insulator photonic wires," Opt. Express. **14**, 3853 (2006), http://www.opticsinfobase.org/abstract.cfm?URI=oe-14-9-3853 .
32. A. C. Turner, C. Manolatou, B. S. Schmidt, M. Lipson, M. A. Foster, J. E. Sharping, A. L. Gaeta, "Tailored anomalous group-velocity dispersion in silicon channel waveguides," Opt. Express **14**, 4357 (2006), http://www.opticsinfobase.org/abstract.cfm?URI=oe-14-10-4357.
33. G. P. Agrawal, *Nonlinear Fiber Optics* (Academic Press, Boston, 1989).
34. J. D. Harvey, R. Leonhardt, S. Coen, G. K. L. Wong, J. C. Knight, W. J. Wadsworth, P. St. J. Russell, "Scalar modulation instability in the normal dispersion regime by use of a photonic crystal fiber," Opt. Lett. **28**, 2225 (2003).
35. T. V. Andersen, K. M. Hilligsoe, C. K. Nielsen, J. Thogersen, K. P. Hansen, S. R. Keidling, J. J. Larsen, "Continuous-wave wavelength conversion in a photonic crystal fiber with two zero-dispersion wavelengths," Opt. Express **12**, 4113 (2004), http://www.opticsinfobase.org/abstract.cfm?URI=oe-13-9-3581.
36. J. Hansryd, A. Andrekson, M. Westlund, J. Li, P. Hedekvist, "Fiber-based optical parametric amplifiers and their applications," IEEE J. Sel. Top. Quantum Electron. **8**, 506 (2002).

#84176 - $15.00 USD Received 15 Jun 2007; revised 13 Aug 2007; accepted 13 Aug 2007; published 24 Sep 2007

37. M. A. Foster, K. D. Moll, A. L. Gaeta, "Optimal waveguide dimensions for nonlinear interactions," Opt. Express **12**, 2880 (2004), http://www.opticsexpress.org/abstract.cfm?URI=OPEX-12-13-2880.
38. X. Chen, N. C. Panoiu, and R. M. Osgood, Jr., "Theory of Raman-mediated pulsed amplification in silicon-wire waveguides," IEEE J. Quantum Electron. **42**, 160 (2006).
39. C. Koos, L. Jacome, C. Poulton, J. Leuthold, and W. Freude, "Nonlinear silicon-on-insulator waveguides for all-optical signal processing," Opt. Express **15**, 5976 (2007), http://www.opticsinfobase.org/abstract.cfm?URI=oe-15-10-5976.
40. A. Zhang, M. S. Demokan, "Broadband wavelength converter based on four-wave mixing in a highly nonlinear photonic crystal fiber," Opt. Lett. **30**, 2375 (2005).
41. Z. G. Lu, P. J. Bock, J. R. Liu, F. G. Sun, T. J. Hall, "All-optical 1550 to 1310 nm wavelength converter," Electron. Lett. **42**, 937 (2006).
42. V. R. Almeida, R. R. Panepucci, M. Lipson, "Nanotapers for compact mode conversion," Opt. Lett. **28**, 1302 (2003).

1. Introduction

Reducing the power requirements and size of nonlinear optical devices is critical to their implementation in optical systems. Benefiting from a large refractive index, large nonlinear response, and a mature and low-cost fabrication process, silicon has recently emerged as a highly attractive material for nonlinear photonic integration. Compact all-optical devices based on two-photon absorption [1–3], free-carrier dispersion [4, 5], the Raman effect [6–12], and the Kerr effect [1, 2, 13–16] have all been demonstrated in silicon. For parametric processes such as self-phase modulation [1, 13, 14, 17, 18], cross-phase modulation [15, 19, 20], and FWM [21–29] the group-velocity dispersion (GVD) [1, 30–32] is a critical parameter, which defines conditions, for example, for solitonic or non-solitonic behavior and phase-matching [33]. In fact, a pulsed experiment using anomalous-GVD in appropriately scaled silicon waveguides recently demonstrated broad-bandwidth parametric gain via FWM [26]. In experiments, optimization of continuous-wave (CW) FWM in silicon has focused on the waveguide length and free carrier-lifetime [23–25, 27, 29], but little attention has been paid to optimizing phase-matching through GVD [22, 26, 28].

In this paper, we experimentally demonstrate highly broad-band frequency conversion using FWM in silicon nanowavegudies. We demonstrate 3-dB conversion bandwidths as large as 150 nm with peak conversion efficiencies of -9.6 dB. Utilizing a waveguide with low third-order dispersion (TOD) and low GVD, we are able to tune the pump throughout the C-band while maintaining conversion bandwidths > 100 nm. Pumping close to the zero-GVD point of one waveguide, we find the phase-matching bandwidth is determined not only by the GVD but also by the fourth-order dispersion (FOD) [34, 35]. Using higher-order dispersion phase-matching, we convert signals from 1477 nm to 1672 nm with an efficiency of -12 dB. To demonstrate the utility of silicon wavelength converters, we convert a 10-Gb/s NRZ data train across the C-band from 1535 nm to 1566 nm with minimal degradation of the signal quality.

2. Theory

Efficient FWM requires minimal phase-mismatch of the four interacting waves [33, 36]. Considering a degenerate pump and including the effects of cross- and self-phase modulation, this mismatch Δk is given by,

$$\Delta k = 2\gamma P_{pump} - \Delta k_{linear}, \tag{1}$$

where $\gamma = 2\pi n_2/\lambda A_{eff}$ is the effective nonlinearity, n_2 is the nonlinear refractive index, λ is the wavelength of light, A_{eff} is the mode area, P_{pump} is the pump power, $\Delta k_{linear} = 2k_{pump} - k_{signal} - k_{idler}$ is the linear phase-mismatch, and k_{pump}, k_{signal}, and k_{idler} are the pump, signal, and idler propagation constants. Including the effects of dispersion up to fourth-order, the linear

#84176 - $15.00 USD Received 15 Jun 2007; revised 13 Aug 2007; accepted 13 Aug 2007; published 24 Sep 2007

phase-mismatch is approximately given by,

$$\Delta k_{linear} = -\beta_2(\Delta\omega)^2 - \frac{1}{12}\beta_4(\Delta\omega)^4, \tag{2}$$

where $\beta_2 = d^2k/d\omega^2$ is the GVD parameter at the pump wavelength, $\beta_4 = d^4k/d\omega^4$ is the fourth-order dispersion (FOD) parameter at the pump wavelength, and $\Delta\omega$ is the frequency difference between the pump and signal waves. Only the even-order dispersion terms play a role in the phase-mismatch due to the symmetry of the FWM process. A commonly used GVD parameter D is related to β_2 by $D = -2\pi c\beta_2/\lambda^2$. The conversion efficiency G_{idler} is given by [36],

$$G_{idler} = \frac{P^{out}_{idler}}{P^{in}_{signal}} = \left[\frac{\gamma P_{pump}}{g}\sinh(gL)\right]^2, \tag{3}$$

where

$$g = \left[\gamma P_{pump}\Delta k_{linear} - (\Delta k_{linear}/2)^2\right]^{\frac{1}{2}} \tag{4}$$

is the parametric gain parameter, P_{pump} is the pump power, P^{out}_{idler} is the output power in the idler wave, P^{in}_{signal} is the input power of the signal wave, and L is the interaction length. The maximum efficiency G^{max}_{idler} occurs when $\Delta k = 0$ and is given by,

$$G^{max}_{idler} = \sinh^2(\gamma P_{pump}L). \tag{5}$$

The conversion bandwidth can be estimated as the bandwidth for which $|\Delta kL| < \pi$ [33]. This definition provides a bandwidth slightly larger than the 3-dB bandwidth. In the small-gain limit, $2\gamma P_{pump}L << \pi$, this bandwidth is independent of the pump power, and including solely the effects of GVD, the conversion bandwidth Ω_{FWM} is approximately given by,

$$\Omega_{FWM} \approx \left[\frac{4\pi}{\beta_2 L}\right]^{\frac{1}{2}}. \tag{6}$$

The conversion bandwidth is inversely proportional to the square root of the product of β_2 and the interaction length. By reducing either of these parameters, the bandwidth is extended. The choice of length is also dependent on the desired conversion efficiency, and for embedded silicon waveguides, γ is five orders of magnitude larger than conventional single-mode fibers [37–39]. Using pump powers on the order of 100 mW, this yields conversion efficiencies of -10 dB, using an interaction length of only 1 cm. Such short interaction lengths allow conversion bandwidths in silicon waveguides to be much larger than those of silica optical fibers, assuming comparable GVD. Much work has focused on GVD optimization in specially designed highly nonlinear optical fibers achieving conversion bandwidths > 100 nm [40, 41]. Achieving these maximal bandwidths in silicon will likewise require careful design of the waveguide geometry for minimal GVD.

3. Dispersion and phase-matching

The material GVD of silicon is large and normal near 1550 nm, with a value of approximately $D = -1{,}000$ ps/(nm·km). The large index contrast of silicon-on-insulator waveguides (3.5 to 1.5) allows for a large waveguide contribution to the dispersion for highly confining waveguides. It was recently shown that by finely adjusting the waveguide dimensions, the GVD near 1500 nm can be varied to any value from large and anomalous [i.e. $D = 5{,}000$ ps/(nm·km)] to large and normal [i.e $D = -15{,}000$ ps/(nm·km)] [30–32]. In this paper, we consider silicon waveguides of uniform 300-nm height with widths ranging from 500 nm to 750 nm. The GVD

#84176 - $15.00 USD Received 15 Jun 2007; revised 13 Aug 2007; accepted 13 Aug 2007; published 24 Sep 2007

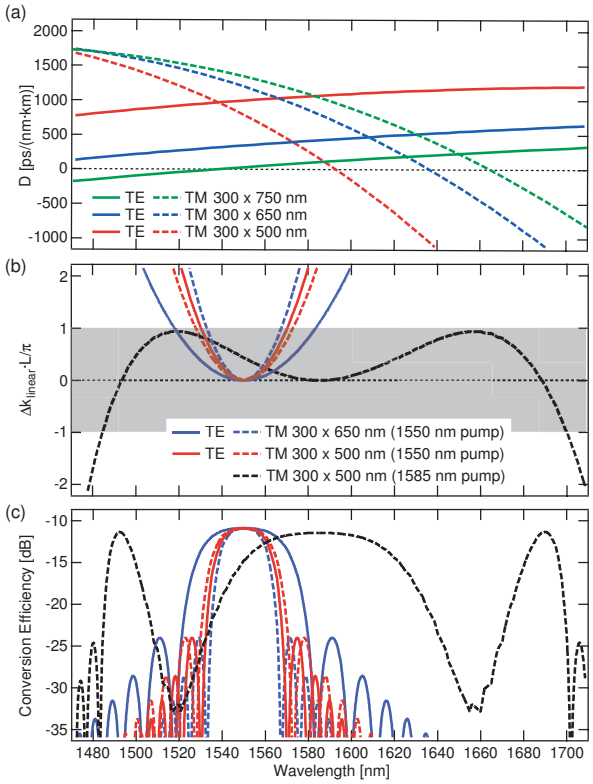

Fig. 1. (a) Simulated group-velocity dispersion D of the TE and TM modes for three of the waveguide cross-sections used in this investigation, (b) the acquired phase mismatch after 1-cm of propagation, and (c) the predicted conversion efficiency for 100-mW pump power and 1-cm interaction length. All curves assume a pump wavelength of 1550 nm except the black curve which has a pump wavelength of 1585 nm. In the small-gain limit, the conversion bandwidth corresponds to the range of wavelengths for which the magnitude of this linear mismatch is less than π, as indicated by the grey region in (b). The waveguides with the lowest GVD at the pump wavelength have the largest conversion bandwidth. When the pump is tuned near the zero-GVD point to 1585-nm (dashed black curve), fourth-order dispersion adds two additional phase matching points away from the pump wavelength.

of three of these waveguides for the TE and TM polarization modes are shown in Fig. 1(a). The range of sizes yields GVD values from $D = 50$ ps/(nm·km) to $D = 1,000$ ps/(nm·km) at 1550 nm. For a pump at 1550 nm and for a 1-cm interaction length, the linear phase-mismatch for the 500-nm wide and 650-nm wide waveguides are shown in Fig. 1(b). As explained in the previous section, in the small-gain limit the conversion bandwidth is approximately the wavelength range over which the magnitude of this linear mismatch is less than π. For TE (TM) polarization the larger (smaller) waveguide has the lowest magnitude of GVD. Correspondingly, the conversion bandwidth for the TE (TM) polarization is largest in the larger (smaller) waveguide. Assuming a 100-mW CW pump and a 1-cm interaction length, the predicted conversion bandwidths are shown in Fig. 1(c). Under these conditions, conversion efficiencies of -10 dB are expected with bandwidths approaching 60 nm.

If the pump wavelength is tuned near the zero-GVD point of a waveguide, the FOD plays an important role in the phase-mismatch. For TM polarization in the 300-nm by 500-nm waveguide, a pump wavelength of 1585 nm demonstrates this behavior. The phase mismatch under

#84176 - $15.00 USD Received 15 Jun 2007; revised 13 Aug 2007; accepted 13 Aug 2007; published 24 Sep 2007

these conditions is shown in Fig. 1(b), in which two phase-matching regions appear; one extremely broad region near the pump is due to the GVD, and a second set further from the pump is due to FOD. The position of the FOD phase-matched region can be calculated from Eq. (2) and is given by,

$$\Delta\omega = \sqrt{\frac{12\,|\beta_2|}{|\beta_4|}}, \tag{7}$$

assuming β_2 and β_4 are of opposite sign. The predicted conversion efficiency for a 100-mW pump and 1-cm interaction length is shown in Fig. 1(c). Such a scheme should allow wavelength conversion over a 200-nm range with efficiencies of approximately -10 dB.

The analysis of this section neglects the nonlinear losses of two-photon absorption (TPA) and free-carrier absorption (FCA) present in silicon waveguides. For a pump power of 100-mW and a propagation length of 1-cm the losses due to TPA and FCA is calculated to be less than 0.7 dB and therefore will have a small effect on the conversion efficiency. Furthermore, in this small-gain limit the conversion bandwidth depends solely on the GVD and will not depend on nonlinear absorption, pump power, or variations in the effective nonlinearity of the waveguides. However, for higher pump powers or effective nonlinearities, the nonlinear losses will lead to saturation of the peak conversion efficiency.

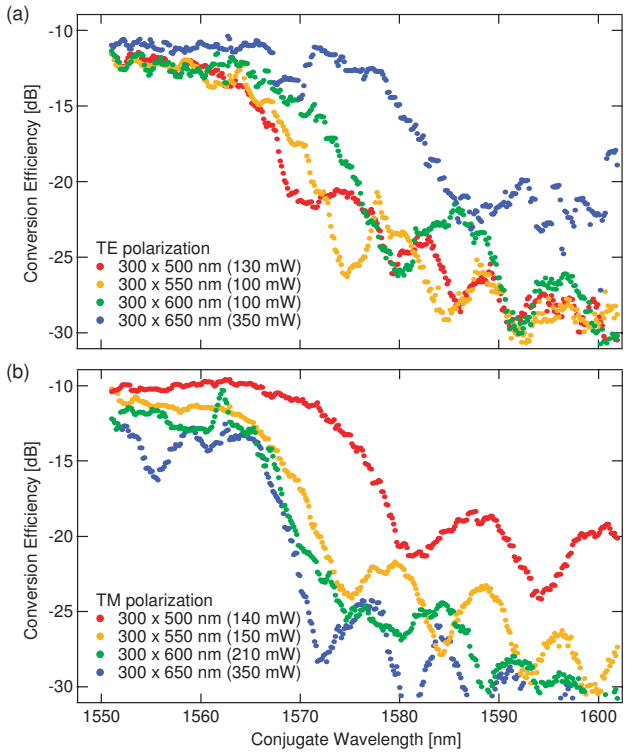

Fig. 2. Experimentally measured conversion efficiency in the (a) TE and (b) TM polarization modes of the four waveguides with the pump wave at 1550 nm. The TM mode of the smallest waveguide and the TE mode of the largest waveguide have the lowest GVD magnitude and consequently have the largest conversion bandwidths.

#84176 - $15.00 USD Received 15 Jun 2007; revised 13 Aug 2007; accepted 13 Aug 2007; published 24 Sep 2007

4. Experiment

The embedded silicon waveguides in this investigation are fabricated as previously described [26, 32]. Five cross-sectional sizes are utilized which are all 300-nm tall with widths from 500 nm to 750 nm. The four waveguides with widths from 500 nm to 650 nm are 1.8-cm long and have linear propagation losses ranging from 1 to 1.5 dB/cm. The 750-nm wide waveguide is 2-cm long and has a 3-dB/cm propagation loss. We use two tunable lasers to form the pump and signal waves. The pump wave is amplified in an EDFA and subsequently filtered and combined with the signal in a wavelength-division multiplexer. The two waves are coupled into the silicon waveguide using a tapered-lens fiber and an inverse-taper mode converter [42]. A fiber polarization controller before the tapered-lens fiber allows for selection of TE or TM polarization. The waves exiting the waveguide are collimated, filtered by a polarizer, and collected with a single-mode fiber or free-space power meter for analysis. The coupling loss was measured using a low power input (less than 5 mW) to avoid nonlinear loss mechanisms and comparing to the output power corrected for the propagation loss. We measured coupling losses ranging from -7 dB to -13 dB and obtained better coupling in waveguides with larger dimensions.

The experimentally measured conversion efficiencies for the 500 to 650-nm-wide waveguides pumped at 1550 nm are shown in Fig. 2. For comparison with previous research [23–27, 29], we define conversion efficiency as the converted power exiting the waveguide with the pump on divided by the signal power exiting the waveguide with the pump off. For these measurements, the power inside the waveguide ranges from 100 mW to 350 mW due to the respective coupling efficiencies for each of the waveguides. For TE polarization (see Fig. 2(a)), we see an increase in conversion bandwidth with increased cross-sectional waveguide size due to the corresponding decrease in GVD magnitude and we observe a maximum conversion efficiency of -10.4 dB and a maximum 3-dB conversion bandwidth of 58 nm, including the symmetric lobe to the short wavelength side. In comparison, for TM polarization (see Fig. 2(b)) we see an increase in the 3-dB conversion bandwidth with decreased cross-sectional waveguide size which is also due to a corresponding decrease in GVD magnitude and we observe a maximum conversion efficiency of -9.6 dB and a maximum 3-dB conversion bandwidth of 48 nm, including the symmetric lobe. For both polarizations the conversion bandwidth is critically dependent on the magnitude of GVD in this small-gain limit. Using the waveguides and

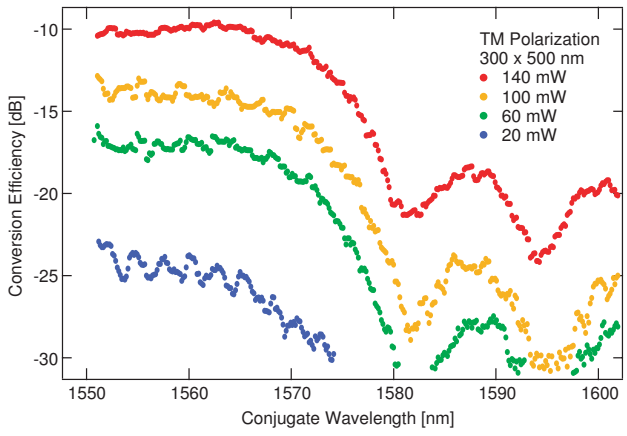

Fig. 3. Experimentally measured conversion efficiency for various pump powers in the TM polarization of the 300-nm by 500-nm waveguide. While the maximum efficiency is highly dependent on pump power, the conversion bandwidth is not.

#84176 - $15.00 USD Received 15 Jun 2007; revised 13 Aug 2007; accepted 13 Aug 2007; published 24 Sep 2007

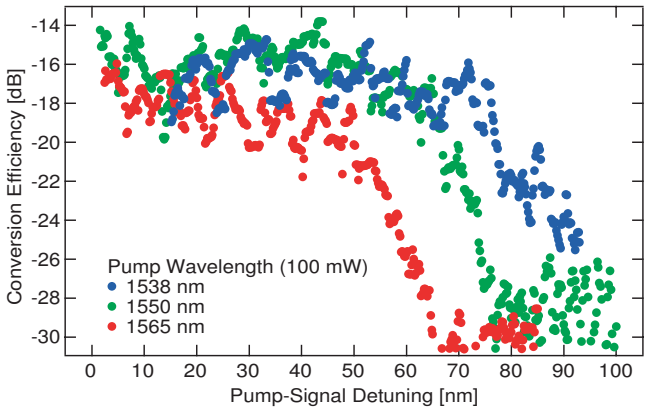

Fig. 4. Experimentally measured conversion efficiency for the TE mode of the 300-nm by 750-nm waveguide for three pump wavelengths spanning the C-band. The 3-dB conversion bandwidth remains $>$ 100 nm for signal wavelengths tuned relative to these pump wavelengths demonstrating that any C-band signal can be converted to any other C-band wavelength by tuning the pump wavelength.

polarizations with lowest magnitude of GVD allows us to convert across the entire C-band with conversion efficiencies higher than -11 dB.

The dependence of conversion efficiency on pump power is shown in Fig. 3 for the TM polarization in the 300-nm by 500-nm waveguide. Although the conversion bandwidth is not highly dependent on pump power, the conversion efficiency is determined primarily by the coupled pump power. Interestingly, the conversion efficiency does not saturate for the powers investigated here which indicates that with improved coupling efficiency higher conversion efficiencies can be expected. This result is consistent with our observation of minimal nonlinear losses for the power levels used in this experiment.

While third-order dispersion (TOD) does not influence the FWM bandwidth, it does limit the ability to tune the pump wavelength and maintain a large bandwidth. The tunability of the pump wavelength is an important factor for wavelength conversion of a fixed signal to an arbitrary wavelength. By choosing the TE mode of the 300-nm by 750-nm waveguide, which exhibits low TOD and low GVD, we are able to choose three pump wavelengths throughout the C-band

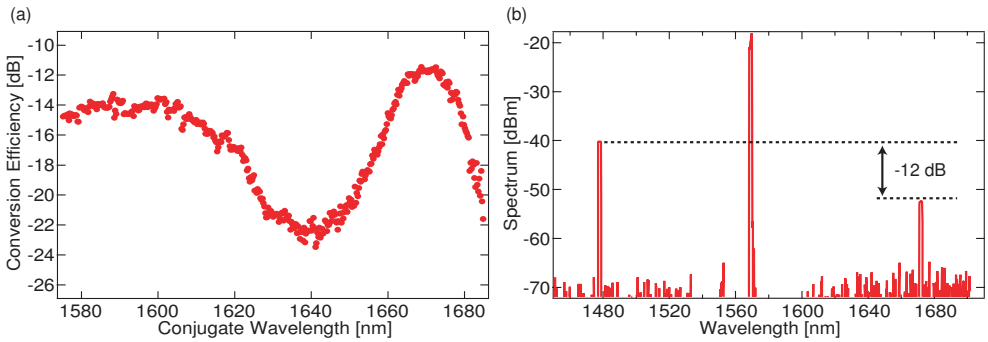

Fig. 5. (a) Experimentally measured conversion efficiency pumping at 1568 nm in the TM mode of the 300-nm by 500-nm waveguide. This pump wavelength is near the zero-GVD point of the waveguide allowing phase-matching through fourth-order dispersion further from the pump. (b) This fourth-order phase matching yields conversion across four telecommunication bands from 1477 nm to 1672 nm with -12 dB efficiency

#84176 - $15.00 USD Received 15 Jun 2007; revised 13 Aug 2007; accepted 13 Aug 2007; published 24 Sep 2007

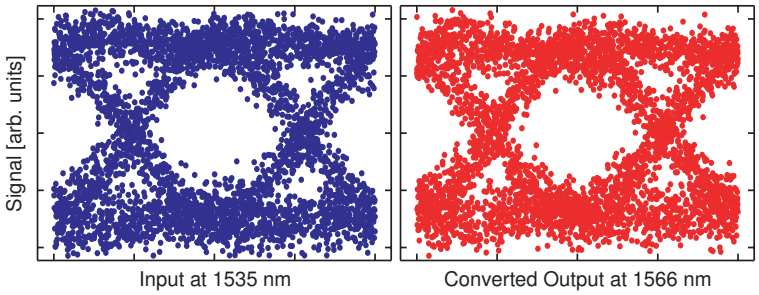

Fig. 6. Eye diagrams associated with conversion of a 10-Gb/s signal from 1535 nm (blue) to 1566 nm (red). The converted output shows minimal degradation of the data quality.

while maintaining a 3-dB conversion bandwidth > 100 nm as the signal is tuned relative to these pump wavelengths (see Fig. 4). Since the zero-GVD point occurs to the short wavelength side of our pump-tuning range, the largest 3-dB conversion bandwidth of 150 nm occurs for the shortest pump wavelength. We were unable to tune the signal to within 12-nm of the 1538-nm pump due to the WDM used to combine the two waves. However, similar conversion is clearly expected since the phase-mismatch will only decrease for these small detunings. The ability to tune the pump throughout the C-band while maintaining large conversion bandwidths demonstrates that we can convert any C-band signal to any other C-band wavelength by solely tuning the pump wavelength.

To observe larger signal-idler detunings, we tune the pump wavelength to 1568 nm, close to the zero-GVD wavelength of the TM mode in the 300-nm by 500-nm waveguide. Figure 5(a) shows the conversion efficiency for this pump wavelength, and its spectral dependence is determined by both GVD and FOD, due to the proximity of the zero-GVD point. The low GVD magnitude yields a 3-dB conversion bandwidth of 100 nm near the pump wavelength, including the symmetric lobe to shorter wavelengths. Fourth-order dispersion leads to a second 40-nm wide region of efficient conversion further from the pump wavelength, including the symmetric lobe. As illustrated in Fig. 5(b), this region enables conversion across four telecommunications bands from 1477 nm (S-band) to 1672 nm (U-band) with an efficiency of -12 dB.

To demonstrate that the FWM process in silicon nanowaveguides does not appreciably degrade an optical signal, we convert 10-Gb/s NRZ data from 1535 nm to 1566 nm using the TM-polarization mode of the 300-nm by 500-nm waveguide. The choice of a 1535-nm input is limited by the EDFA bandwidth and not the conversion bandwidth of the process, as shown in Fig. 2. For this measurement, the converted signal is detected with no post amplification. Figure 6(a) shows the eye diagrams of the input signal (1535 nm) and the converted output (1566 nm), which is measured using a $2^{31} - 1$ pseudo-random bit sequence. Both eye diagrams are measured with an input signal of -20 dBm. Although time-dependence to the loss mechanisms such as free-carrier absorption or thermal effects may be a concern, minimal degradation of the signal quality occurs on the converted output as has been demonstrated over narrower bandwidths [25, 27, 29]. Since the pump is CW, any nonlinear absorption mechanisms will not be time dependent and thus will not degrade the signal.

5. Conclusion

We demonstrate continuous-wave four-wave mixing in silicon nanowaveguides over an extremely broad bandwidth, allowing for conversion across four telecommunications bands from 1477 nm to 1672 nm. These demonstrations are enabled by combining the large effective nonlinearity of these waveguides (five orders of magnitude larger than single-mode fiber) with

#84176 - $15.00 USD Received 15 Jun 2007; revised 13 Aug 2007; accepted 13 Aug 2007; published 24 Sep 2007

the ability to engineer the GVD through the dominating contribution of waveguide dispersion. These broad bandwidths illustrate the ability to tune the GVD in designing silicon parametric wavelength converters. The combination of large conversion bandwidths and low pump powers allow the porting of existing parametric optical processing technology from silica fibers to photonic integrated circuits.

Acknowledgments

We gratefully acknowledge discussions with David F. Geraghty. This work is funded by the Center for Nanoscale Systems, supported by the NSF and the New York State Office of Science, Technology and Academic Research, and the DARPA DSO Slow-Light Program. M.A.F. acknowledges support through the IBM Graduate Fellowship Program.

#84176 - $15.00 USD Received 15 Jun 2007; revised 13 Aug 2007; accepted 13 Aug 2007; published 24 Sep 2007